

ZHOU, Y., WANG, S., XIE, Y., ZHU, T. and FERNANDEZ, C. 2024. An improved particle swarm optimization-least squares support vector machine-unscented Kalman filtering algorithm on SOC estimation of lithium-ion battery. *International journal of green energy* [online], 21(2), pages 376-386. Available from: <https://doi.org/10.1080/15435075.2023.2196328>

An improved particle swarm optimization-least squares support vector machine-unscented Kalman filtering algorithm on SOC estimation of lithium-ion battery.

ZHOU, Y., WANG, S., XIE, Y., ZHU, T. and FERNANDEZ, C.

2024

This is an Accepted Manuscript of an article published by Taylor & Francis in International Journal of Green Energy on 30.03.2023, available at:

<http://www.tandfonline.com/10.1080/15435075.2023.2196328>

An improved particle swarm optimization-least squares support vector machine-unscented Kalman filtering algorithm on SOC estimation of lithium-ion battery

Yifei Zhou^a, Shunli Wang^a, Yanxin Xie^a, Tao Zhu^a, and Carlos Fernandez^b

^aSchool of Information Engineering, Engineering and Technology Center, Southwest University of Science and Technology, Mianyang, China; ^bSchool of Pharmacy and Life Sciences, Robert Gordon University, Aberdeen, UK

ABSTRACT

For real-time monitoring and safe control of electrical vehicles, it is important to accurately estimate the state of charge of lithium-ion batteries. A combined data-driven modeling approach based on Least squares support vector machine based on particle swarm optimization and unscented Kalman filter is proposed to obtain a better state of charge estimation accuracy. In this article, least squares support vector machine is used to establish the nonlinear connection between current, voltage, and SOC, and the parameters of least squares support vector machine are optimized by particle swarm optimization to improve the accuracy of voltage estimation, and the state and measurement equations are established by Least squares support vector machine in unscented Kalman filter for SOC estimation. The experimental results show that the maximum voltage error for the voltage prediction made with the PSO optimized model is 0.5 V. The maximum SOC error under various working situations is similarly kept to 0.5%, which is a significant improvement compared to the traditional algorithm. The above data show that the PSO considerably increases the precision of the Least squares support vector machine, as well as the estimation accuracy of the voltage and SOC, demonstrating the effectiveness of the model.

KEYWORDS

Lithium-ion batteries; state of charge; unscented Kalman filter; particle swarm optimization; least squares support vector machine; electrical vehicles

1. Introduction

Due to the extended cycle life, lack of memory while charging, and lack of pollutants during production and recycling, lithium-ion batteries (LIBs) are extensively utilized in new energy electric vehicles (EVs) and lithium battery technology. Although LIBs have many advantages, they can also have disadvantages, such as their electrochemical nature being active and the side reactions during charging and discharging tend to heat up and generate heat, so there are certain safety risks (Nizam et al. 2020). Hence, to operate an electrical system, a safe battery management system (BMS) is required (Gabbar, Othman, and Abdussami 2021). The BMS may offer the driver dynamic control over the energy storage system together with precise battery operating status information. One of the most crucial battery management system indications is state of charge (SOC), and proper calculation of SOC may increase the battery's utilization and extend its useable life. Because of the acquisition equipment's precision problem and outside variables like load, voltage, temperature, etc., it is challenging to establish a precise model to estimate SOC. It is significant to construct a trustworthy and precise model in order to estimate SOC for EV security and stability.

Several SOC estimate algorithms have recently been proposed to improve the accuracy of SOC estimation (Plett 2019). The most commonly used methods include the open-circuit voltage method, the internal impedance method, the ampere-time integration method, and methods based on different circuit models (Meng et al. 2017). The ampere-time integration method makes it simple to estimate SOC online, but error accumulation due to timing issues, battery capacity, and current sensor issues lower the accuracy of SOC estimates. Open-circuit voltage (OCV) and SOC are roughly linear in terms of OCV estimation, and SOC estimate is quite accurate. The method does not apply to online SOC estimates for EV, though, as the battery must run for a considerable amount of time to achieve a stable OCV. SOC can also be measured using the internal resistance method (Sun, Li, and You 2020). But to finish the SOC calculation, several impedance experiments are needed, and the SOC estimation results are not very good (Rodrigues, Munichandraiah, and Shukla 2000). To reduce errors, many methods based on models have been studied and electrochemical models have been proposed by Smith *et al* (Smith, Rahn, and Wang 2007), they may produce a variety of LIB properties, but they have drawbacks, such as sophisticated models, challenging computations, difficult parameter acquisition, and bad practices. In (Di Domenico, Fiengo, and Stefanopoulou 2008), proposed a Kalman filtering algorithm based on the electrochemical model, established a model for averaging data based on the chemistry of the battery, and successfully estimated the SOC, but the accuracy of the SOC was overly reliant on the averaging model. Spagnol *et al* (Spagnol, Rossi, and Savaresi 2011) studied SOC estimation using the Kalman filter (KF) and showed that SOC has good accuracy. However, there is a trade-off problem, where the accuracy decreases when the estimator converges quickly, and conversely, a high accuracy estimator makes the convergence very slow. The experimental results show that both the extended

Kalman filter (EKF) and the unscented Kalman filter (UKF) are effective at estimating the SOC for the nonlinear system. However, EKF ignores the higher-order element when expanding the equation using the Taylor technique, which results in inaccurate SOC estimation (Plett 2004). The findings show that UKF, which employs the unscented transformation (UT) to turn the approximation linear function into the probability density function, is more precise and simpler to design than EKF (Wan and Van Der Merwe 2001). However, human experience determines the noise covariance in UKF, which could cause the filtering results to diverge.

The battery model estimation performance has recently been improved by the application of an increasing number of machine learning methods. The most extensively researched data-driven approach, the neural network (NN), has had great success in SOC estimate (Charkhgard and Farrokhi 2010). Also based on NN many variants have been generated, corresponding to SOC estimation with the same considerable accuracy, such as fuzzy neural network (Xu, Wang, and Chen 2012), dual neural network (Dang et al. 2016), and back propagation (BP) neural network (Guo, Zhao, and Huang 2017). To lessen the effect of battery degradation on SOC estimate, Kang *et al* (Kang, Zhao, and Ma 2014) presented the radial basis function (RBF) NN model. In order to estimate SOC, Reference (Chaoui and Ibe-Ekeocha 2017) proposed a combined model based on UKF and neural network, experimental findings indicate that this approach is capable of producing an accurate SOC calculation in a variety of experimental circumstances. However, the NN method tends to enter the local optimum when obtaining parameters. A novel method built on statistical learning theory is support vector machine (SVM) (Anton et al. 2013; Hansen and Wang 2005). Looking for the least amount of structural risk enhances the machine's capacity for learning and generalization. The results show that the model may solve nonlinear problems and produce better results by using least square-support vector machine (LS-SVM), which replaces the inequality constraint in SVM with an equation constraint (Zhang et al. 2019).

This research proposes a data-driven model for lithium battery SOC estimation using the PSO-LS-SVM algorithm. Although the conventional LS-SVM can handle nonlinear, high-dimensional, and small-sample problems, when dealing with nonlinear issues, the choice of kernel function parameters can have a significant effect on the classification outcomes. Therefore, by building a PSO-LS-SVM data-driven model, PSO is used to choose the ideal parameters of the kernel function, and the algorithm is used to establish the nonlinear connection between voltage, current, and SOC for parameter identification, and the voltage of model output is contrasted with the voltage of experimentally measured to identify the precise of the PSO algorithm, and the PSO algorithm has collaborative search (directing the search with both individual local information and group global information), more rapid convergence, easier to leapfrog local optimal information, etc. SOC estimation using the PSO-LS-SVM method to construct a new state equation and measurement equation of UKF, and the viability and accuracy of this improved data-driven model are confirmed.

The structure of this paper is as follows. In the second section, the algorithm used in the data-driven model combined with the mathematical formula will be analyzed in detail. The principle of integrating PSO and LSSVM is presented. The third section uses the model to analyze the battery data under different working conditions and verifies the model between the PSO algorithm parameter identification results and the voltage data obtained by the experiment. The experimental data are carefully analyzed, and a comprehensive comparison between the SOC calculated using the enhanced UKF algorithm and the SOC obtained through ampere-hour integration is made. The conclusion section concludes this work by summarizing the findings.

2. Mathematical analysis

2.1. Particle swarm optimization algorithm

The particle swarm optimization algorithm (PSO) is proposed by Kennedy *et al* (Kennedy and Eberhart 1995) an algorithm for population-based searches that simulates the social behavior of flocks of birds. To order to avoid errors caused by empirical and random choices, the particle swarm optimization algorithm is chosen to optimize the parameters of the kernel function in this paper (Stighezza, Bianchi, and De Munari 2021). PSO is an algorithm that continuously searches for the best solution while considering various possible results. The global ideal solution can be obtained using the present optimal value, and the fitness is used to assess the quality of the optimal solution (De Oca et al. 2009). By referring to the current ideal value, it can determine the global ideal solution. Each particle represents a solution that has a velocity and position vector. In the d -dimensional search space, the position and velocity of the i -th particle can be represented. Individuals are referred to as particles in the PSO algorithm and are flown in hyperdimensional space (Poli, Kennedy, and Blackwell 2007). PSO is a search process based on particle swarm optimization, which is defined as the potential solution of the problem being optimized in the d -dimensional search space and maintains its past best position and the best position of all particles as well as the velocity. Each time the evolution is generated, the particle information is combined to adjust the speed of its components in various dimensions and used to calculate the position of the new particle. Particles change states in the multi-dimensional search space until they reach equilibrium or optimum states or exceed computational limits. For any particle i , the position vector is $X_i=(x_{i1},x_{i2}, \dots ,x_{id})$, and $V_i=(v_{i1},v_{i2}, \dots ,v_{id})$. The ideal position for each particle is unique.

Figure 1, is evident from the PSO algorithm. The initial values need to be set first, and then the optimal parameters can be derived by the continuous movement of the particles to LS-SVM.

In this algorithm, the following formula is used for iteration:

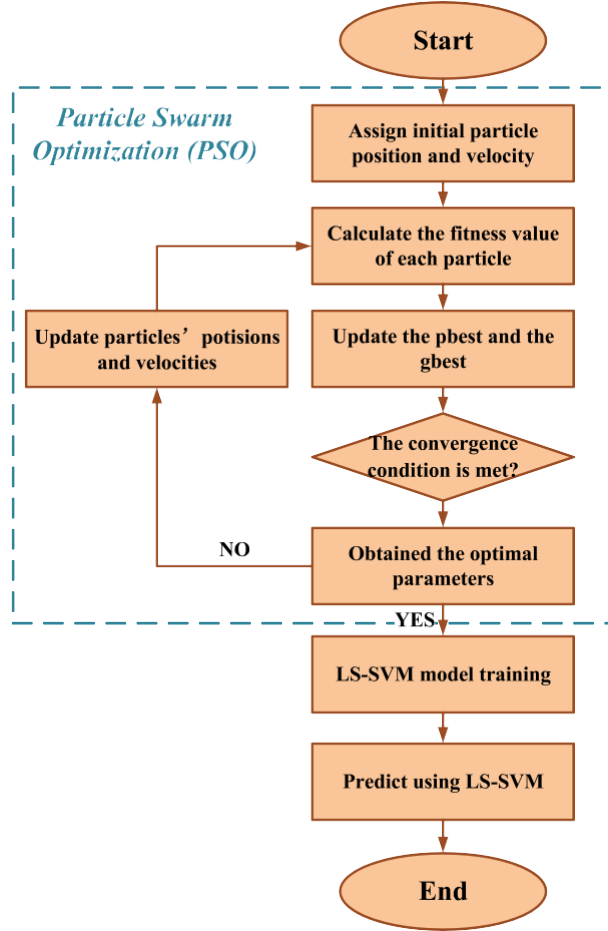


Figure 1. The process of particle swarm optimization.

$$\begin{aligned}
 v_{ij}^{k+1} &= wv_{ij}^k + c_1r_{1j}(p_{ij}^k - x_{ij}^k) + c_2r_{2j}(p_{gj}^k - x_{ij}^k) \\
 x_{ij}^{k+1} &= x_{ij}^k + v_{ij}^{k+1}
 \end{aligned} \tag{1}$$

Where r_{1j} and r_{2j} are random numbers from 0 to 1, c_1 and c_2 are the learning factors, and their values are typically between 0 and 2, and w is the inertia weighting factor.

In this study, a PSO-LS-SVM system for battery SOC estimation is proposed (Li et al. 2019). The goal of this system is to automatically solve the selection of LS-SVM models while maximizing the LS-SVM regression accuracy by predicting the ideal values of kernel parameters and regularization parameters. A stochastic, parallel optimization algorithm is the PSO algorithm. Its benefits include speedier convergence, the algorithm's simplicity and ease of programming and implementation, and the fact that it does not require the optimized function to have differentiable, derivable, continuous, or other qualities (Li et al. 2019). To discover the best set of parameters for the LS-SVM and increase classification accuracy, PSO was used to optimize LS-SVM parameters σ and λ .

2.2. Optimized least squares support vector machine algorithm

Support vector machines (SVM) are binary classification models that can be distinguished from perceptrons by having a fundamental model that is a linear classifier defined by maximizing the interval on the feature space, SVM also has kernel tricks, which make them into nonlinear classifiers (Yan 2020). The optimization algorithm to solve convex quadratic programming is the learning algorithm of SVM. The fundamental principle of SVM learning is to find the separated hyperplane with the biggest geometric separation that appropriately divides the training data set. There is an infinite number of hyperplanes for sets of data that are linearly divided, but the geometrically maximally spaced separating hyperplanes is unique (Adaikkappan and Sathiyamoorthy 2022).

Since the SVM algorithm is difficult to implement on large- scale training samples, a modified SVM was chosen for the experiment. When it comes to tackling small-sample learning problems, a data-driven algorithm called LS-SVM which is built on statistical theory has some specific advantages. It can successfully avoid the local optimal solution of the neural network and overcome the influence of dimensionality (Jiabo et al. 2020). The best feature of LS-SVM is to integrate the quadratic programming problem into a linear equation problem by changing the SVM inequality constraint to an equation constraint and using the training error squared to replace the slack variable. This greatly increases the accuracy and efficiency of the model eigen-value optimization (Dilmen and Beyhan 2017). The LS-SVM model can be constructed for any set of nonlinear samples with known inputs and outputs by selecting the appropriate non- linear transformation inside the following equation:

$$f(x) = w \cdot \varphi(x_k) + b \quad (2)$$

Where $\varphi(x_k)$ is the mapping function, w is the regression function's coefficient, and b is the error value. The following minimal objective can be created using the structural risk minimization principle:

$$\begin{cases} \min J(w, e) = \frac{1}{2} \omega^T \omega + \frac{1}{2} \gamma \sum_{k=1}^N e_k^2 \\ \text{s.t.} \quad y_k = \omega^T \phi(x_k) + b + e_k \end{cases} \quad (3)$$

Where e_k is the error variable, b is the error value, and γ is the regularization parameter, commonly known as the penalty factor.

To solve the optimization problem, the Lagrangian multiplier method is introduced:

$$L(w, b, e; \alpha) = J(w, e) - \sum_{k=1}^N \alpha_k \{ w^T \phi(x_k) + b + e_k - y_k \} \quad (4)$$

Where α is the LaGrange multiplier.

Take the partial derivative of w , b , e_k , α_k concerning the function of L , respectively, and make $L(w; b; e; \alpha)$. The formula is as follows:

$$\begin{cases} w = \sum_{k=1}^N \alpha_k \phi(x_k) \\ \sum_{k=1}^N \alpha_k = 0 \\ 2e^k = \alpha_k \\ w^T \phi(x_k) + b + e_k - f(x_k) = 0 \end{cases} \quad (5)$$

If $K(x_i; x_j)$ satisfies Mercer's condition, then (3) and (4) can be combined to get the following equations:

$$f(x_k) = \sum_{k=1}^{\infty} \alpha_k K(x, x_k) + b \quad (6)$$

The kernel function is significant in the LS-SVM. The main goal of kernel functions is to break the dimensionality curse by using them to map linearly inseparable samples into high-dimensional space. It is possible to divide the mapped samples linearly. A classification plane created in the high-dimensional space is then used to split the samples of the two classes. When building a classifier, the kernel function is critical since it determines the structure of the feature space (Chen et al. 2018). For the data noise, the radial basis function provides excellent anti-interference properties, and convergence can be achieved without further assumptions on the objective function (Gutmann 2001).

$$K(x_i, x_j) = e^{-\frac{\|x_i - x_j\|^2}{2\sigma^2}} \quad (7)$$

As a result, LS-SVM used the value of SOC and current as the input vectors.

Figure 2 shows the terminal voltage estimated using PSO-LS-SVM. The input vector of the LS-SVM uses the Current $I(k)$ and SOC (k) of the lithium battery measured at instant k , and $V(k)$ is the corresponding voltage value at moment k . The relationship between SOC, voltage, and current is established using LS-SVM due to the nonlinear relationship between the internal parameters of LIBs.

$$V_k = \sum_{k=1}^{\infty} \alpha_k K(\text{SOC}_k, i_k) + b \quad (8)$$

The two most crucial LS-SVM model parameters to recognize kernel parameter σ and the penalty factor λ . The PSO method is used in this study to find the optimal local parameters and the ideal global parameters in order the optimal parameters (λ, σ) .

2.3. SOC estimation based on LS-SVM-UKF

SOC is defined as the proportion of the battery's remaining capacity to its nominal capacity, which is expressed as:

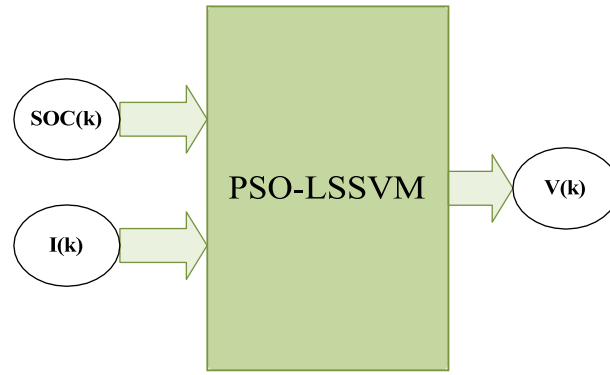


Figure 2. PSO-LS-SVM parameter identification process.

$$\text{SOC} = \text{SOC}_0 - \frac{\int_0^t \eta i(\theta) d\theta}{Q_0} \quad (9)$$

Where SOC_0 is the initial value, η is the discharge and charging efficiency, $i(\theta)$ is the current at the θ sample time, and Q_0 is the rated capacity of the LIBs.

The discretization of Equation (10) can be used as the state equation in the KF, where x_k represents the SOC at the sampling k time.

$$x_k = x_{k-1} - \frac{\eta}{Q_0} \Delta t \cdot i_k \quad (10)$$

In this study, the Unscented Kalman Filter (UKF) was utilized, which is accurate to the third order, in the sense of a Taylor series expansion for any nonlinearity (Bhuvana, Unterrieder, and Huemer 2013).

The unscented transform (UT), a statistical method, is directly applied in UKF. The sigma points are a collection of precisely selected sample points used in UT, serving as the representation of a Gaussian distribution. These sigma points accurately represent the mean and covariance of GRVs that are propagated through a nonlinear function. And prognostics Xiong *et al* (Xiong et al. 2014) proposed a multi-time scale-based EKF to achieve a joint estimation of parameters and SOC for LIBs. He *et al* (He et al. 2013) and Zhang *et al* (Zhang, Liu, and Fang 2009) utilized UKF to estimate SOC with root mean square error (RMSE) of less than 5% for SOC estimation. In this paper, the state and measurement equations for SOC estimation are established based on the principle of UKF using the RBF kernel function equation of LS-SVM and the equation for calculating the ampere-time integral of SOC. Equation (7) and Equation (9) are employed, respectively, as measurement equations and the state equation of UKF. Measurement noise and state noise are introduced into Equation (11) as a result of errors in the model generation processes and data measurement.

$$\begin{cases} x_k = f(x_{k-1}, i_k) + q_k = x_{k-1} - \frac{\eta}{Q_0} \Delta t \cdot i_k + q_k \\ y_{k-1} = V_{k-1} + r_k = \sum_{k=2}^{\alpha} \alpha_k K(x_{k-1}, i_{k-1}) + b + r_k \end{cases} \quad (11)$$

Where the state vectors and measurement vectors, x_k , and y_{k-1} , are defined as the SOC value at time k and the estimated voltage at time $k-1$, respectively. State noise and measurement noise, respectively, are denoted by Q_k and r_k .

For a nonlinear discrete-time system (Julier, Uhlmann, and Durrant-Whyte 2000), the state equation and measurement equation are described:

$$\begin{cases} x_k = f(x_{k-1}, u_k) + q_k \\ y_k = h(x_k, u_k) + r_k \end{cases} \quad (12)$$

Where f and h , respectively, stand for the measurement model and the nonlinear process model. The unmeasurable state vector is represented by the vector x_k , the control input vector by the vector u_k , the observed output vector by the vector y_k , the system noise vector by the vector r_k , and the measurement noise vector by the vector w_k .

$$\begin{aligned} Q_k &= E[q_k \cdot q_k^T] \\ R_k &= E[r_k \cdot r_k^T] \end{aligned} \quad (13)$$

Both q_k and r_k are zero-mean Gaussian white sequences that are not correlated, and Q_k and R_k , respectively, represent their covariance. The mathematical formula UKF is shown as follows:

(1) Initialization:

$$\begin{aligned} \bar{x}_0 &= E[x_0] \\ P_0 &= E[(x_0 - \bar{x}_0)(x_0 - \bar{x}_0)^T] \end{aligned} \quad (14)$$

(2) Augmented state vector and covariance matrix are:

$$\begin{aligned} x^a &= [x^T, q^T, r^T]^T \\ \bar{x}_0^a &= [\bar{x}_0^T, 0, 0]^T \\ P_0^a &= E[(x^a - \bar{x}_0^a)(x^a - \bar{x}_0^a)^T] = \text{diag}(P_0, Q_0, R_0) \end{aligned} \quad (15)$$

(3) Generating sigma points:

$$\begin{cases} \chi_0 = \bar{x}_{k-1} \\ \chi_i = \bar{x}_{k-1} + (\sqrt{(N+\lambda)P_k})_i, i = 1, \dots, N \\ \chi_i = \bar{x}_{k-1} - (\sqrt{(N+\lambda)P_k})_i, i = N+1, \dots, 2N \end{cases} \quad (16)$$

Where $(\sqrt{(N+\lambda)P_k})_i$ is the i -th column of the matrix. In Equation (16) the parameter λ is the scale:

$$\lambda = a^2(N+k) - N \quad (17)$$

Additionally, the computation of weighted coefficients is provided:

$$\begin{cases} \omega_0^m = \frac{\lambda}{\lambda+N} \\ \omega_i^m = \frac{\lambda}{2(\lambda+N)}, i = 1, \dots, 2N \end{cases} \quad (18)$$

$$\begin{cases} \omega_0^c = \frac{\lambda}{\lambda+N} + (1 - \alpha^2 + \beta) \\ \omega_i^c = \frac{\lambda}{2(\lambda+N)}, i = 1, \dots, 2N \end{cases} \quad (19)$$

(4) First updating the sigma point and covariance:

$$\begin{aligned} \chi_{k|k-1} &= f(\chi_{k-1}) \\ \bar{x}_{k|k-1} &= \sum_{i=0}^{2n} \omega_i^m \chi_{i,k|k-1}^* \\ P_{k|k-1} &= \sum_{i=0}^{2n} \omega_i^c (\chi_{i,k|k-1}^* - \bar{x}_{k|k-1})(\chi_{i,k|k-1}^* - \bar{x}_{k|k-1})^T + Q_{k-1} \end{aligned} \quad (20)$$

Measurement Update:

$$\begin{cases} y_{i,k|k-1} = h(\chi_{i,k|k-1}) \\ \bar{y}_{k|k-1} = \sum_{i=0}^{2n} \omega_i^m y_{i,k|k-1} \\ P_{y,k} = \sum_{i=0}^{2n} \omega_i^c (y_{i,k|k-1} - \bar{y}_{k|k-1})(y_{i,k|k-1} - \bar{y}_{k|k-1})^T + R_{k-1} \\ P_{xy,k} = \sum_{i=0}^{2n} \omega_i^c (\chi_{i,k|k-1} - \bar{x}_{k|k-1})(y_{i,k|k-1} - \bar{y}_{k|k-1})^T \end{cases} \quad (21)$$

(5) Calculating the Kalman gain:

$$K_k = P_{xy,k}(P_{y,k})^{-1} \quad (22)$$

(6) Second updating the states and covariance:

$$\begin{aligned} \bar{x}_k &= \bar{x}_{k|k-1} + K_k(y_k - \bar{y}_{k|k-1}) \\ P_k &= P_{k|k-1} - K_k P_{y,k} K_k^T \end{aligned} \quad (23)$$

The whole SOC estimate flowchart is provided in this paper and is based on the aforementioned algorithm. This flowchart is shown in Figure 3.

As can be seen from the flowchart in Figure 3, a complete process is divided into three steps. First, the experimentally obtained real SOC, current, and voltage values into the LS- SVM model optimized by PSO and use radial basis function estimation to obtain the simulated voltage values. Second, the LS-SVM is used as a framework to establish the states and measure equations for the voltages. Finally, SOC estimation was performed using the data input to the UKF algorithm.

3. Experimental verification

In this section, the relevant data of lithium-ion batteries, such as current, voltage, and SOC, will be obtained experimentally under different working conditions. The data of HPPC, DST, and BBDST operating conditions were obtained. In addition, three types of evaluation criteria are used in this article, which includes Root means square error (RMSE) and mean absolute error (MAE), and relative error. The mathematical definitions of the above evaluation criteria are as follows:

$$\begin{aligned}
RMSE &= \sqrt{\frac{\sum_k^N (y_{act} - y_{est})^2}{N}} \\
MAE &= \frac{\sum_k^N |y_{act} - y_{est}|}{N} \\
error &= y_{act} - y_{est}
\end{aligned}
\tag{24}$$

Where y_{act} is the actual value and y_{est} is the estimated value.

3.1. PSO program parameters selection

Before setting the parameters for the particle swarm optimization process based on the LS-SVM algorithm, the data must first be normalized and the training sample space must be constructed. Following the input of the optimal parameters, LS-SVM outputs the results of the prediction. The particle swarm optimization algorithm produces the most optimal values for relevant parameters (Castanho et al. 2022). In Figure 4, the blue curve depicts how rapidly the PSO method converges, indicating that the PSO is highly quick at quickly and precisely determining the optimal solution, which aids in determining the best LS-SVM parameters and increases the model's validity and accuracy.

To effectively converge the search space in a specific area when tackling practical optimization problems, it is frequently preferable to start with a global search before switching to a local fine search to get high-precision results. Therefore, the strategy of adaptive adjustment is proposed, that is, the value decreases linearly as the iteration progresses (Lai et al. 2018). According to a straightforward and widely-used linear change strategy method, the particle swarm algorithm has strong global convergence ability in the early stage and strong local convergence ability in the later stage as the number of iterations increases and the inertia weight drops.

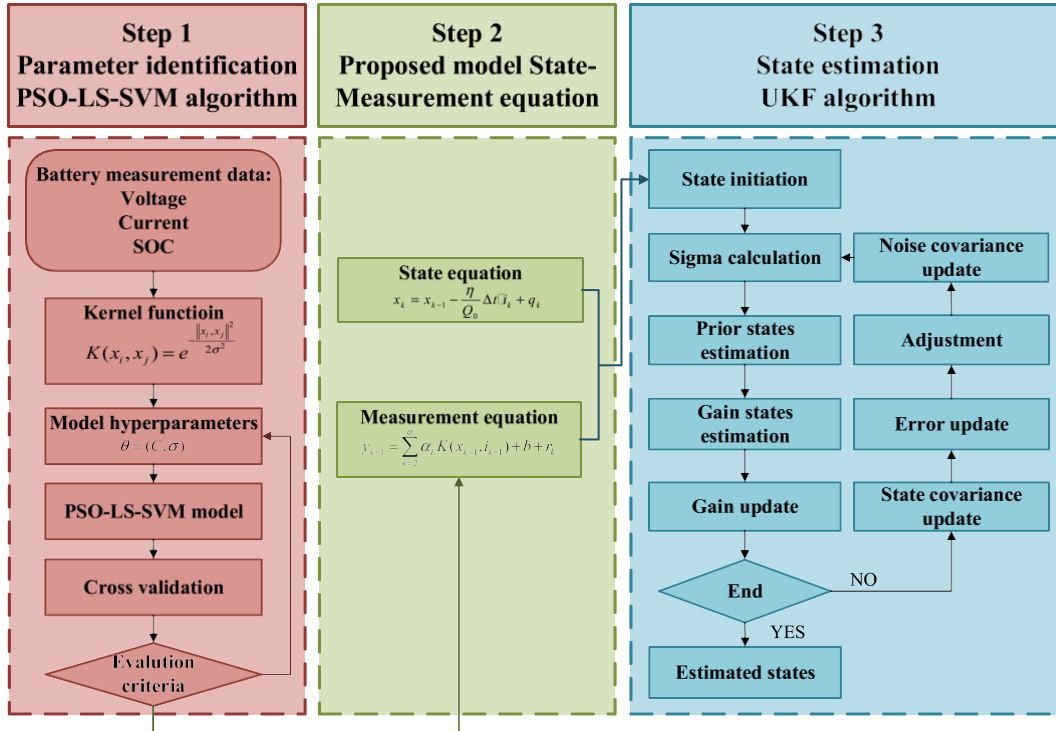


Figure 3. The process of PSO-LS-SVM-UKF.

The PSO parameter's local search ability is represented by the parameter $c1 = 1.5$ in the computer program, characterizing the impact of a single extreme value on the current solution, and the global search ability is represented by the parameter $c2 = 1.8$, characterizing the impact of a global extreme value on the current solution. Smaller populations are more susceptible to local optimums; bigger populations can improve convergence and discover the global optimum solution more quickly, but each

iteration will require more computing power. Therefore, 20 particles are chosen as the particle population size and there will be 20 tests. According to the real circumstances during the optimization process, the number of iterations needs to be modified; if the number is too low, the solution is unstable, and if the number is too high, the procedure is time-consuming and needless. As a result, 100 experiments are picked for the number of iterations.

3.2. SOC estimation under HPPC condition The experimental test is conducted using a ternary lithium-ion battery with a rated capacity of 45Ah and a nominal voltage of 3.7 V. The test platform is a BTS200-100-104 battery test device, and software installed at the PC control terminal is used to regulate the battery charging and discharging conditions to correspond with the test device. All of the experiments in this study are conducted at a constant temperature of 25 degrees Celsius to prevent the impact of temperature variability on the parameters and OCV of the battery.

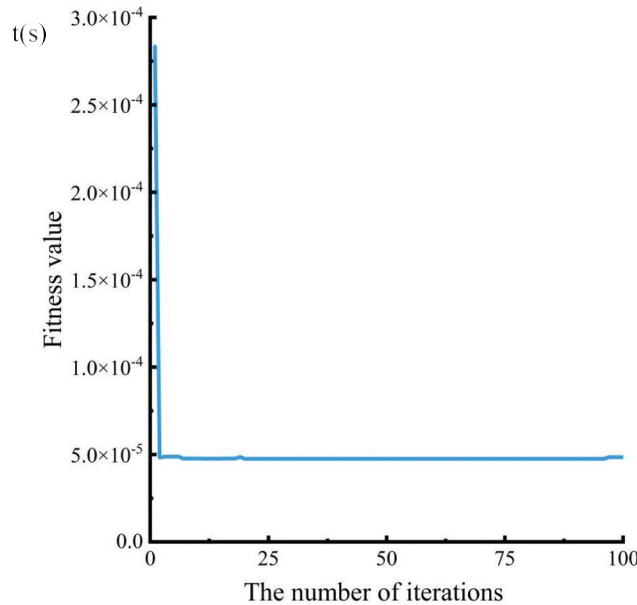
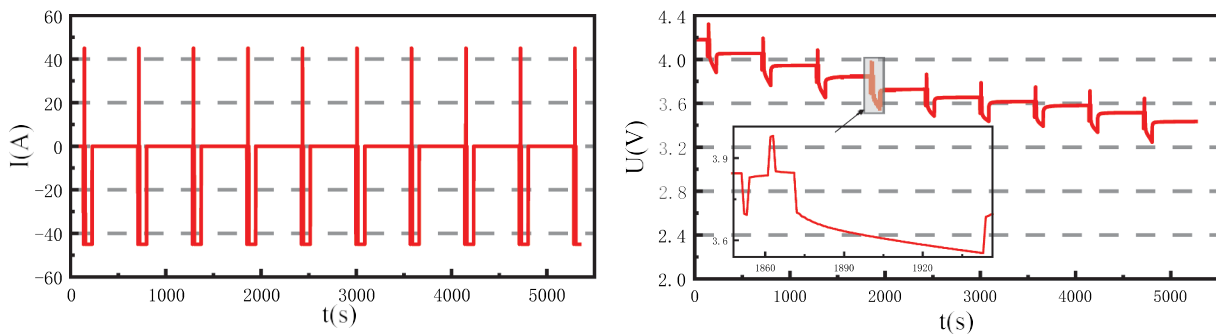


Figure 4. The fitness curve.

Figure 5 shows the current and voltage curves under HPPC conditions. The experimental results are shown in Figure 6, it is clear that the PSO-LS-SVM has a higher accuracy for voltage estimation. Can see that the estimation capability of PSO-LS-SVM outperforms the original LS-SVM, and its maximum absolute error is only 0.091 V. The corresponding RMSE decreases by 62.6% and the MAE further decreases from 0.586% to 0.379%. Indicating that PSO successfully optimizes the LS-SVM to improve the accuracy and stability of voltage estimation.

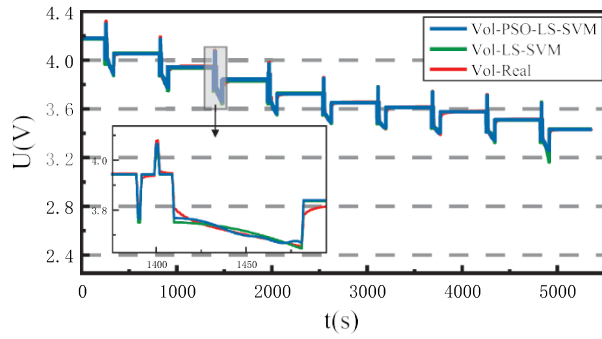
In Figure 7, the estimated voltage obtained by PSO-LS-SVM is brought into the UKF algorithm for comparison with the real voltage, and the state equation and measurement equation in Equation (11) is used to finally derive the UKF estimated SOC value. It can be seen that the results of SOC estimation are more satisfactory, the maximum absolute error of SOC is 0.179%. The RMSE and MAE are 0.039% and 0.023% respectively in a good range.



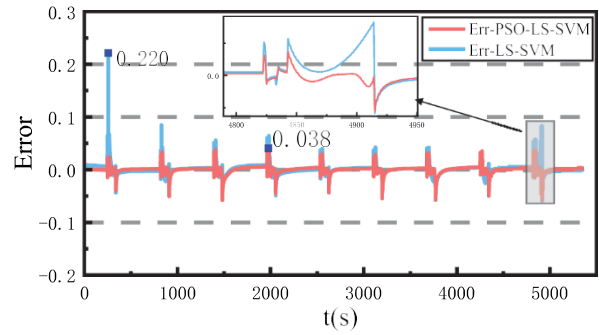
(a) The real current value

(b) The real voltage value

Figure 5. The real experiment data of HPPC condition.

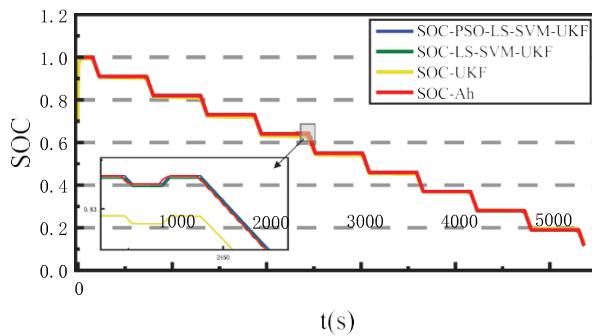


(a) The voltage comparison

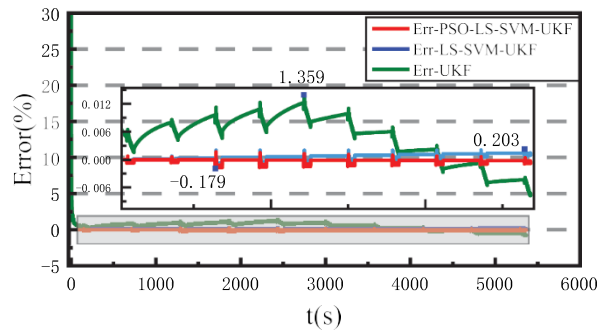


(b) The error of voltage estimation

Figure 6. The voltage estimation in HPPC condition.



(a) The SOC comparison

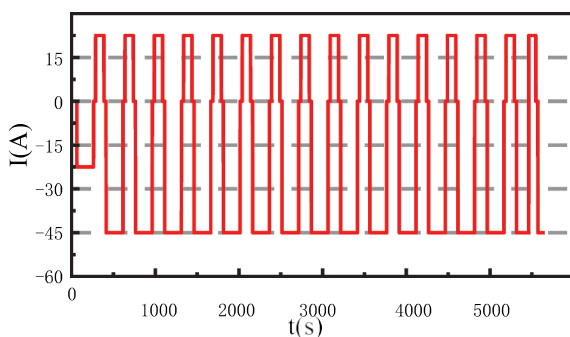


(b) The error of SOC estimation

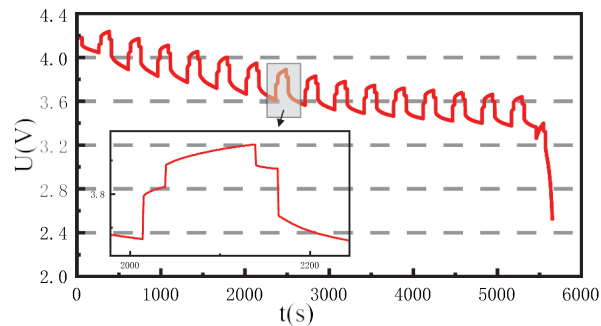
Figure 7. The SOC estimation in HPPC condition.

3.2. SOC estimation under DST condition

Figure 8 shows the current and voltage curves under DST conditions. As can be seen in Figure 9, the maximum relative error of the PSO-LS-SVM voltage estimation under DST is 0.472 V, the RMSE is reduced by 27.7% and only 3.833% compared to LS-SVM, and the MAE is reduced by 19.4% and only 2.061%. In Figure 10, the maximum error of 0.052% in the SOC estimation for the DST condition is the most excellent. And its RMSE and MAE are 0.020% and 0.016% respectively also in the better range.



(a) The real current value



(b) The real voltage value

Figure 8. The real experiment data of DST condition.

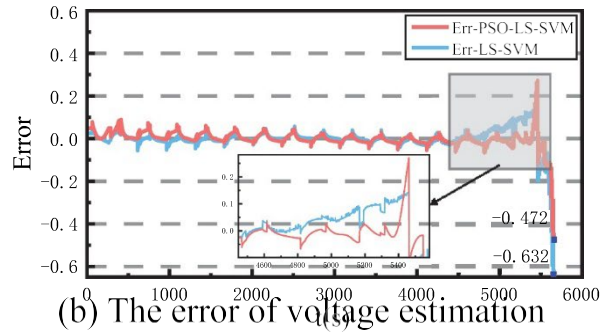
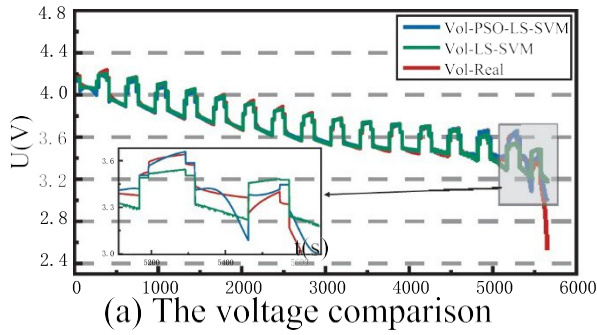


Figure 9. The voltage estimation in DST condition.

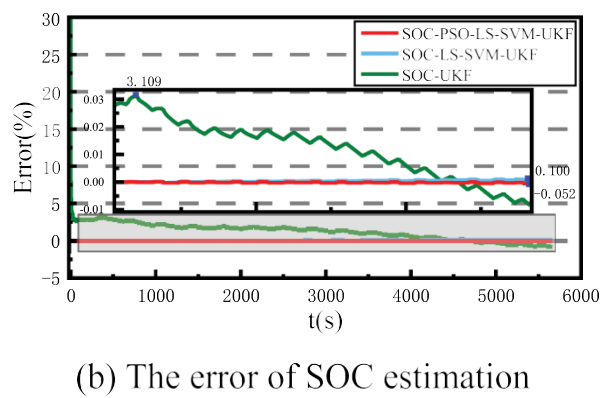
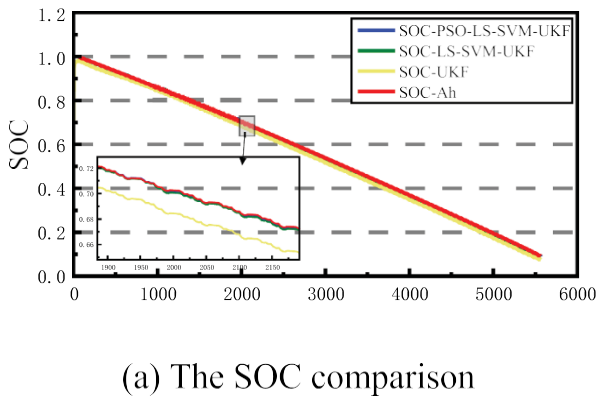


Figure 10. The SOC estimation in DST condition.

3.3. SOC estimation under BBDST condition

Figure 11 shows the current and voltage curves under BBDST conditions. As can be seen in Figure 12, the maximum relative error of PSO-LS-SVM voltage estimation for BBDST condition is 0.046 V, which is 87.2% lower than LS-SVM, and its RMSE is 86.1% lower than LS-SVM by only 0.208%, and MAE is 70.5% lower by only 0.232%, so it can be seen that PSO is the most obvious optimization for BBDST condition. In Figure 13, the maximum error of SOC estimation in BBDST condition is 0.301% in the middle position, and the RMSE and MAE are 0.113% and 0.095% respectively, which are in the reasonable range.

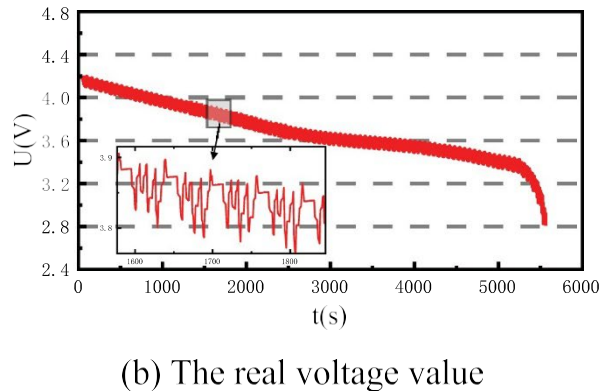
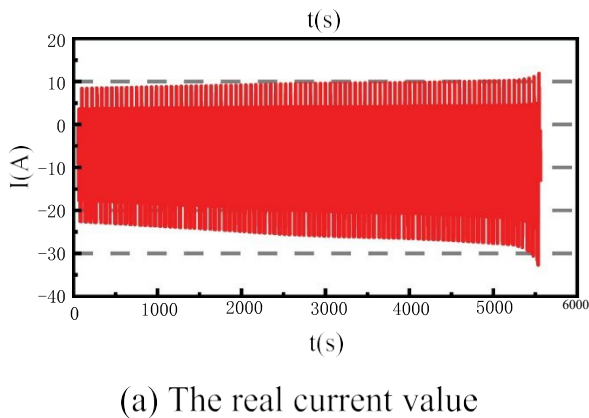
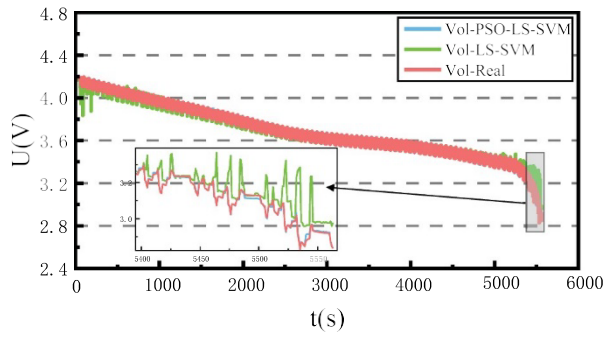
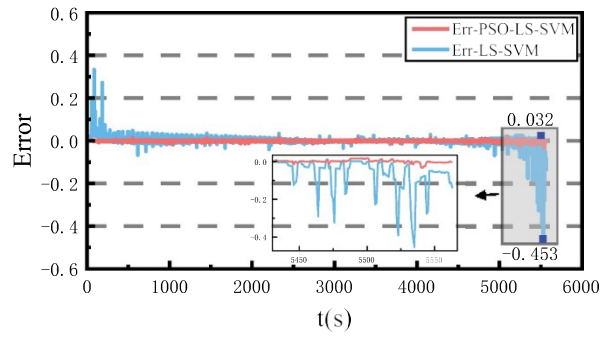


Figure 11. The experiment data of BBDST condition.

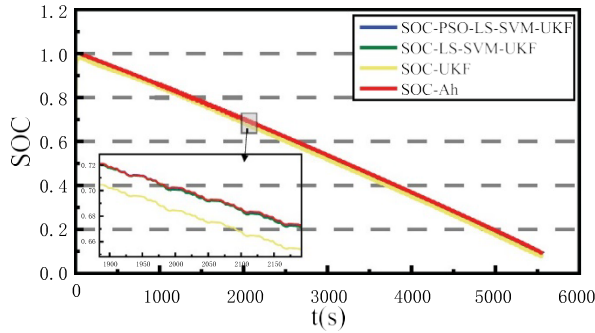


(a) The voltage comparison

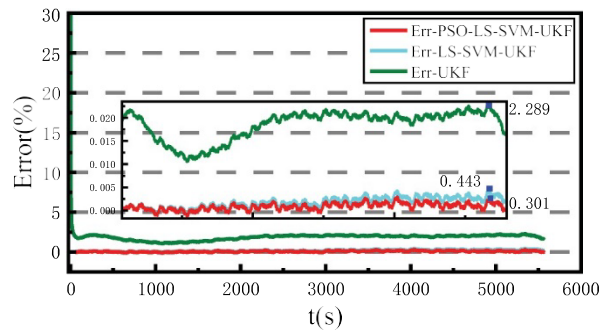


(b) The error of voltage estimation

Figure 12. The voltage estimation in BBDST condition.



(a) The SOC comparison



(b) The error of SOC estimation

Figure 13. The SOC estimation in BBDST condition.

In Table 1, it can be shown that the PSO algorithm can considerably enhance the estimation capability of LS-SVM and shows an extremely good performance in voltage estimation. The improvement in voltage estimation is no less than 50% under different operating conditions. And the RMSE and MAE values are always kept in a reasonable and good range.

As can be seen in Table 2, SOC estimation using PSO algorithm optimized voltage data can also further improve the accuracy of SOC. The SOC estimate under different working conditions can be guaranteed within 0.5%. And the values of MAE and RMSE are also guaranteed at a low level of about 0.2%, indicating that the tracking ability of the estimation process is strong.

Table 1. Comparison of experimental error analysis of different algorithms.

Work Condition	Model	Maximum Absolute Error (V)	RMSE (%)	MAE (%)
HPPC	LS-SVM	0.484	1.874%	0.586%
	PSO-LS-SVM	0.091	0.698%	0.379%
DST	LS-SVM	0.632	5.300%	2.556%
	PSO-LS-SVM	0.472	3.833%	2.061%
BBDST	LS-SVM	0.453	2.216%	0.787%
	PSO-LS-SVM	0.032	0.208%	0.232%

Table 2. Comparison of experimental error analysis of different working conditions.

Work Condition	Model	Maximum Absolute Error (%)	RMSE (%)	MAE (%)
HPPC	UKF	1.359%	0.882%	0.632%
	LS-SVM-UKF	0.203%	0.084%	0.073%
	PSO-LS-SVM-UKF	0.179%	0.039%	0.023%
DST	UKF	3.109%	1.713%	1.304%
	LS-SVM-UKF	0.100%	0.050%	0.043%
	PSO-LS-SVM-UKF	0.052%	0.020%	0.016%
BBDST	UKF	2.289%	1.961%	1.873%
	LS-SVM-UKF	0.443%	0.207%	0.178%
	PSO-LS-SVM-UKF	0.301%	0.113%	0.095%

4. Conclusion

In this study, a data-driven model is built to accomplish high accuracy state of charge estimation under various operating conditions. This model provides new energy vehicles with a more accurate remaining mileage projection, promoting safe driving. The root means square error distribution for particle swarm optimized least squares support vector machine charge state estimation under complex operating conditions is 0.039%, 0.020%, and 0.113%, which are more than half of the conventional UKF. In conclusion, this data-driven model and method have been shown to improve lithium-ion battery state of charge estimate. To ensure that drivers are operating new energy vehicles safely, it is essential to monitor the status of the vehicle in real time. The theoretical groundwork for battery condition monitoring is provided in this paper. However, in the real driving process, the temperature is complex and changes and future research directions will focus on considering the impact of real-time temperature changes on the battery charging state.

References

- Adaikkappan, M., and N. Sathiyamoorthy. 2022. Modeling, state of charge estimation, and charging of lithium-ion battery in electric vehicle: A review. *International Journal of Energy Research* 46 (3):2141–65. doi:10.1002/er.7339.
- Anton, J. C. A., P. J. Garcia Nieto, C. Blanco Viejo, and J. A. Vilan Vilan. 2013. Support vector machines used to estimate the battery state of charge. *IEEE Transactions on Power Electronics* 28 (12):5919–26. doi:10.1109/TPEL.2013.2243918.
- Bhuvana, V. P., C. Unterrieder, and M. Huemer. 2013. Battery internal state estimation: A comparative study of non-linear state estimation algorithms. 2013 IEEE Vehicle Power and Propulsion Conference (VPPC), 15-18 October 2013, Beijing, China. IEEE. doi:10.1109/VPPC.2013.6671666.
- Castanho, D., M. Guerreiro, L. Silva, J. Eckert, T. Antonini Alves, Y. D. S. Tadano, S. L. Stevan, H. V. Siqueira, and F. C. Corrêa. 2022. Method for SoC estimation in lithium-ion batteries based on multiple linear regression and particle swarm optimization. *Energies* 15 (19):6881. doi:10.3390/en15196881.
- Chaoui, H., and C. C. Ibe-Ekeocha. 2017. State of charge and state of health estimation for lithium batteries using recurrent neural networks. *IEEE Transactions on Vehicular Technology* 66 (10):8773–83. doi:10.1109/TVT.2017.2715333.
- Charkhgard, M., and M. Farrokhi. 2010. State-of-charge estimation for lithium-ion batteries using neural networks and EKF. *IEEE Transactions on Industrial Electronics* 57 (12):4178–87. doi:10.1109/TIE.2010.2043035.
- Chen, Z., M. Sun, X. Shu, R. Xiao, and J. Shen. 2018. Online state of health estimation for lithium-ion batteries based on support vector machine. *Applied Sciences* 8 (6):925. doi:10.3390/app8060925.
- Dang, X., L. Yan, K. Xu, X. Wu, H. Jiang, and H. Sun. 2016. Open-circuit voltage-based state of charge estimation of lithium-ion battery using dual neural network fusion battery model. *Electrochimica acta* 188:356–66. doi:10.1016/j.electacta.2015.12.001.
- De Oca, M. A. M., T. Stutzle, M. Birattari, and M. Dorigo. 2009. Frankenstein's PSO: A Composite Particle Swarm Optimization Algorithm. *IEEE Transactions on Evolutionary Computation* 13 (5):1120–32. doi:10.1109/TEVC.2009.2021465.
- Di Domenico, D., G. Fiengo, and A. Stefanopoulou. 2008. Lithium-ion battery state of charge estimation with a Kalman filter based on a electrochemical model. 2008 IEEE International Conference on Control Applications, 03-05 September, San Antonio, TX, USA. IEEE. doi:10.1109/CCA.2008.4629639.
- Dilmen, E., and S. Beyhan. 2017. A novel online LS-SVM approach for regression and classification. *IFAC-Papersonline* 50 (1):8642–47. doi:10.1016/j.ifacol.2017.08.1521.
- Gabbar, H. A., A. M. Othman, and M. R. Abdussami. 2021. Review of battery management systems (BMS) development and industrial standards. *Technologies* 9 (2):28. doi:10.3390/technologies9020028.
- Guo, Y., Z. Zhao, and L. Huang. 2017. SoC estimation of lithium battery based on improved BP neural network. *Energy Procedia* 105:4153–58. doi:10.1016/j.egypro.2017.03.881.
- Gutmann, H. -M. 2001. A radial basis function method for global optimization. *Journal of Global Optimization* 19 (3):201–27. doi:10.1023/A:1011255519438.
- Hansen, T., and C. -J. Wang. 2005. Support vector based battery state of charge estimator. *Journal of Power Sources* 141 (2):351–58. doi:10.1016/j.jpowsour.2004.09.020.
- He, W., N. Williard, C. Chen, and M. Pecht. 2013. State of charge estimation for electric vehicle batteries using unscented Kalman filtering. *Microelectronics Reliability* 53 (6):840–47. doi:10.1016/j.microrel.2012.11.010.
- Jiabo, L., Zhongyu, LI Shengjie, JIAO Min, YE Xinxin, XU. 2020. Lithium- ion state estimation based on feedback least square support vector machine. *Energy Storage Science and Technology* 9 (3):951.
- Julier, S., J. Uhlmann, and H. F. Durrant-Whyte. 2000. A new method for the nonlinear transformation of means and covariances in filters and estimators. *IEEE Transactions on Automatic Control* 45 (3):477–82. doi:10.1109/9.847726.
- Kang, L., X. Zhao, and J. Ma. 2014. A new neural network model for the state-of-charge estimation in the battery degradation process. *Applied Energy* 121:20–27. doi:10.1016/j.apenergy.2014.01.066.
- Kennedy, J. and R. Eberhart. 1995. Particle swarm optimization. Proceedings of ICNN'95-international conference on neural networks, 27 November 1995 - 01 December 1995, Perth, WA, Australia. IEEE. doi:10.1109/ICNN.1995.488968.
- Lai, X., W. Yi, Y. Zheng, and L. Zhou. 2018. An all-region state-of-charge estimator based on global particle swarm optimization and improved extended Kalman filter for lithium-ion batteries. *Electronics* 7 (11):321. doi:10.3390/electronics7110321.
- Li, L. -L., Z. -F. Liu, M. -L. Tseng, and A. S. F. Chiu. 2019. Enhancing the Lithium-ion battery life predictability using a hybrid method. *Applied Soft Computing* 74:110–21. doi:10.1016/j.asoc.2018.10.014.
- Li, R., S. Xu, Y. Zhou, S. Li, J. Yao, K. Zhou, and X. Liu. 2019. *Toward group applications of zinc-silver battery: A classification strategy based on PSO-LSSVM*, Vol. 8, 4745–4753. Piscataway: IEEE Access. doi:10.1109/ACCESS.2019.2962835.
- Meng, J., M. Ricco, G. Luo, M. Swierczynski, D. -I. Stroe, A. -I. Stroe, and R. Teodorescu. 2017. An overview and comparison of online implementable SOC estimation methods for lithium-ion battery. *IEEE Transactions on Industry Applications* 54 (2):1583–91. doi:10.1109/TIA.2017.2775179.
- Nizam, M., H. Maghfiroh, R. A. Rosadi, and K. D. U. Kusumaputri. 2020. Battery management system design (BMS) for lithium ion batteries. AIP Conference Proceedings, 17–18 September 2019, Surakarta, Indonesia. AIP Publishing LLC. doi:10.1063/5.0000649.

- Plett, G. L. 2004. Extended Kalman filtering for battery management systems of LiPB-based HEV battery packs: Part 3. State and parameter estimation. *Journal of Power Sources* 134 (2):277–92. doi:10.1016/j.jpowsour.2004.02.033.
- Plett, G. L. 2019. Review and some perspectives on different methods to estimate state of charge of lithium-ion batteries. *Journal of Automotive Safety and Energy* 10 (3):249.
- Poli, R., J. Kennedy, and T. Blackwell. 2007. Particle swarm optimization. *Swarm Intelligence* 1 (1):33–57. doi:10.1007/s11721-007-0002-0.
- Rodrigues, S., N. Munichandraiah, and A. Shukla. 2000. A review of state-of-charge indication of batteries by means of ac impedance measurements. *Journal of Power Sources* 87 (1–2):12–20. doi:10.1016/S0378-7753(99)00351-1.
- Smith, K. A., C. D. Rahn, and C. -Y. Wang. 2007. Control oriented 1D electrochemical model of lithium ion battery. *Energy Conversion and Management* 48 (9):2565–78. doi:10.1016/j.enconman.2007.03.015.
- Spagnol, P., S. Rossi, and S. M. Savaresi. 2011. Kalman filter SoC estimation for li-ion batteries. 2011 IEEE International Conference on Control Applications (CCA), 28–30 September 2011, Denver, CO, USA. IEEE. doi:10.1109/CCA.2011.6044480.
- Stighezza, M., V. Bianchi, and I. De Munari. 2021. FPGA implementation of an ant colony optimization based SVM algorithm for state of charge estimation in li-ion batteries. *Energies* 14 (21):7064. doi:10.3390/en14217064.
- Sun, L., G. Li, and F. You. 2020. Combined internal resistance and state-of-charge estimation of lithium-ion battery based on extended state observer. *Renewable and Sustainable Energy Reviews* 131:109994. doi:10.1016/j.rser.2020.109994.
- Wan, E. A., and R. Van Der Merwe. 2001. *The unscented Kalman filter*. *Kalman Filtering and Neural Networks* 5:221–80.
- Xiong, R., F. Sun, Z. Chen, and H. He. 2014. A data-driven multi-scale extended Kalman filtering based parameter and state estimation approach of lithium-ion polymer battery in electric vehicles. *Applied Energy* 113:463–76. doi:10.1016/j.apenergy.2013.07.061.
- Xu, L., J. Wang, and Q. Chen. 2012. Kalman filtering state of charge estimation for battery management system based on a stochastic fuzzy neural network battery model. *Energy Conversion and Management* 53 (1):33–39. doi:10.1016/j.enconman.2011.06.003.
- Yan, Q. 2020. SOC prediction of power battery based on SVM. 2020 Chinese Control And Decision Conference (CCDC), 22–24 August, Hefei, China. IEEE. doi:10.1109/CCDC49329.2020.9164245.
- Zhang, L., K. Li, D. Du, C. Zhu, and M. Zheng. 2019. A sparse least squares support vector machine used for SOC estimation of li-ion batteries. *IFAC-Papersonline* 52 (11):256–61. doi:10.1016/j.ifacol.2019.09.150.
- Zhang, F., G. Liu, and L. Fang. 2009. Battery state estimation using unscented Kalman filter. 2009 IEEE International Conference on Robotics and Automation, 12–17 May, Kobe, Japan. IEEE. doi:10.1109/ROBOT.2009.5152745.